PAPER

Signal-Carrier Cooperative DF Relay Using Adaptive Modulation

Kazuhiro KIMURA[†a)], Hiroyuki MIYAZAKI[†], Tatsunori OBARA[†], *Student Members*, *and* Fumiyuki ADACHI[†], *Fellow*

SUMMARY 2-time slot cooperative relay can be used to increase the cell-edge throughput. Adaptive data modulation further improves the throughput. In this paper, we introduce adaptive modulation to single-carrier (SC) cooperative decode-and-forward (DF) relay. The best modulation combination for mobile-terminal (MT)-relay station (RS) and RS-base station (BS) links is determined for the given local average signal-to-noise power ratios (SNRs) of MT-BS, MT-RS and RS-BS links. According to the modulation combination, the ratio of time slot length of the MT-RS link (first time slot) and the RS-BS link (second time slot) is changed. It is shown by computer simulation that the use of adaptive modulation can achieve higher throughput than fixed modulation and reduces by about 9 dB the required normalized total transmit SNR for a 10%-outage throughput of 0.8 bps/Hz compared to direct transmission.

key words: *cooperative decode-and-forward (DF) relay, single-carrier transmission, adaptive modulation*

1. Introduction

In the next generation mobile communication systems, broadband data transmissions are required. Since the uplink communication range is limited in general by the mobile terminal (MT) transmit power, the signal waveform having low peak-to-average power ratio (PAPR) property is desirable. 2-time slot cooperative relay [2], [3] is a well-known technique to extend the uplink communication range. In the first time slot, MT transmits its signal to both a relay station (RS) and a base station (BS). Then, in the second time slot, RS forwards its received signal to BS. BS combines the two signals received in the first and second time slot. There are two types of relay protocol: amplify-and-forward (AF) relay protocol and decod-and-forward (DF) relay protocol [3]. In this paper, the DF relay protocol is considered.

In broadband data transmissions, the channel becomes severely frequency-selective and strong inter-symbol interference (ISI) is produced, thereby the degrading the transmit performance [4]. Orthogonal frequency division multiplexing (OFDM) can cope with the severe channel frequency-selectivity and achieves a good transmission performance. However, OFDM has a drawback of high PAPR. For uplink transmissions, single carrier (SC) transmission is promising due to its lower PAPR property than OFDM. The use of minimum mean square error based frequency-domain equalization (MMSE-FDE) in SC transmission can take advantage of the channel frequency-selectivity and achieves a good transmission performance [5]. Therefore, we have been paying attention to SC cooperative relay.

The throughput achievable by the cooperative DF relay depends on link of MT-BS, MT-RS, and RS-BS. However, the relay approach is most effective when the MT-RS direct link quality is poor (i.e., when an MT is close to the cell-edge). Therefore, the throughput gain of cooperative relay can be upper-limited by the worse link between the MT-RS link and the RS-BS link [3]. The MT-RS link quality may change over time according to the movement of MT. RS must forward the same amount of data in the second time slot (RS-BS link transmission) as that received in the first time slot (MT-RS link transmission). DF protocol can provide better throughput than AF protocol by adapting data modulation (accordingly, by adapting the ratio of first and second time slot lengths) to match the changing condition of two links. Fiding the optimum modulation combination is an important issue in 2-time slot cooperative DF relay.

There have been many studies on adaptive modulation for cooperative DF relay [6]–[10]. In [6], the cooperative diversity with 2-time slot incremental relay using adaptive modulation scheme was proposed. The modulation combination is selected according to a predetermined threshold of channel quality. In [7], the bit error rate (BER)-based selection combining was proposed; the modulation combination is selected that minimizes the BER after the selections combining at BS. In [8], the adaptive modulation for the demodulation-and-forward relay protocol instead of DF relay was proposed, where RS demodulates/re-modulates the received signal without data decision and the selection combining is used at RS. The modulation combination which satisfies the BER requirement at BS is selected. Refs. [9], [10] proposed adaptive modulation for opportunistic DF relay, where adaptive modulation is jointly performed with relay selection. However, in [6]–[10], a frequency-nonselective fading is assumed and therefore, no equalization technique is considered. Furthermore, Refs. [6]–[10] assume the selection combining at BS.

In this paper, we introduce adaptive modulation to 2-time slot uplink SC cooperative DF relay using MMSE-FDE in a frequency-selective fading channel. We consider two diversity combining schemes: MMSE-FDE combining and log-likelihood ratio (LLR) combining, to obtain higher spatial diversity gain than the selection combining. Further-

Manuscript received December 30, 2012.
Manuscript revised July 24, 2013.

[†]The authors are with the Department of Communications Engineering, Graduate School of Engineering, Tohoku University, Sendai-shi, 980-8579 Japan.
a) E-mail: kazuhiro@mobile.ecei.tohoku.ac.jp

DOI: 10.1587/transcom.E97.B.387

more, noting that in broadband SC, the instantaneous signal-to-noise power ratio (SNR) approaches the local average received SNR, the modulation selection is determined based on the local average SNRs of MT-BS, MT-RS, and RS-BS links. According to the modulation combination, the ratio of time slot lengths of the MT-RS link (first time slot) and the RS-BS link (second time slot) is changed.

The rest of this paper is organized as follows. Sect. 2 presents 2-time slot uplink SC cooperative DF relay with adaptive modulation. In Sect. 3, MMSE-FDE at RS and signal combining at BS are described. The computer simulation results are discussed in Sect. 4. Sect. 5 concludes this paper.

2. Cooperative DF Relay with Adaptive Modulation

2.1 Network Model

In this paper, we consider the uplink SC cooperative DF relay with adaptive modulation. Figure 1 illustrates the cooperative DF relay network model. For simplicity, the single-cell with single-user environment is shown. The cell radius is denoted by D. It is assumed that X RSs are located. The distances between MT and BS, between MT and RS, and between RS and BS are denoted by $r_{M\to B}$, $r_{M\to R}$, and $r_{R\to B}$, respectively, where $R \in \{0, 1, \ldots, X-1\}$. We assume that each of channels of MT-BS, MT-RS, and RS-BS links is characterized by the propagation path loss, the shadowing loss, and the symbol spaced L-path frequency-selective fading. The total transmit power P is assumed to be equally allocated between MT and RS, i.e., $P_M = P_R = P/2$, where P_M and P_R are the transmit power at MT and RS, respectively. The RS selection is based on the instantaneous SNR of the worst link between MT-RS and RS-BS. The RS selection is expressed as

$$R = \underset{R' \in (0,1,\ldots,X-1)}{\operatorname{argmax}} \left\{ \min\left(\sum_{l=0}^{L-1} \left| h_{M\to R'}^{(l)} \right|^2 r_{M\to R'}^{-\alpha} 10^{-\frac{\eta_{M\to R'}}{10}}, \sum_{l=0}^{L-1} \left| h_{B\to R'}^{(l)} \right|^2 r_{B\to R'}^{-\alpha} 10^{-\frac{\eta_{B\to R'}}{10}} \right) \right\}, \quad (1)$$

where α denotes the path loss exponent. $\eta_{M\to R'}$ and $\eta_{R'\to B}$ are the independent log-normally distributed shadowing losses with standard deviation σ in dB for the MT-RS and RS-BS links, respectively, and $h_{M\to R'}^{(l)}$ and $h_{R'\to B}^{(l)}$ are the complex-valued lth path gains of MT-RS link and RS-BS link, respectively, with $E\left[\sum_{l=0}^{L-1} \left|h_{M\to R'}^{(l)}\right|^2\right] = 1$ and $E\left[\sum_{l=0}^{L-1} \left|h_{R'\to B}^{(l)}\right|^2\right] = 1$.

2.2 Adaptive Modulation

In this paper, the perfect knowledge of channel state information (CSI) of the MT-BS, MT-RS, and RS-BS links is assumed to be available at BS. The best modulation combination is predetermined for each set of the MT-BS, MT-RS, and RS-BS link CSIs and is stored in a look-up-table at BS. Then, BS informs both MT and RS the modulation to use.

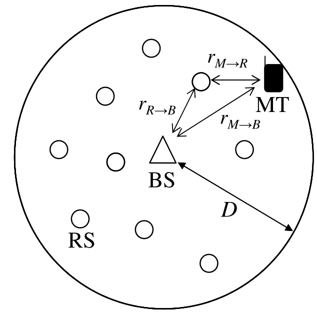

Fig. 1 Relay network model.

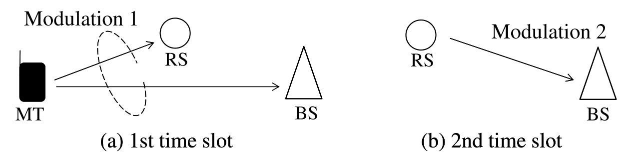

Fig. 2 Uplink cooperative DF relay protocol.

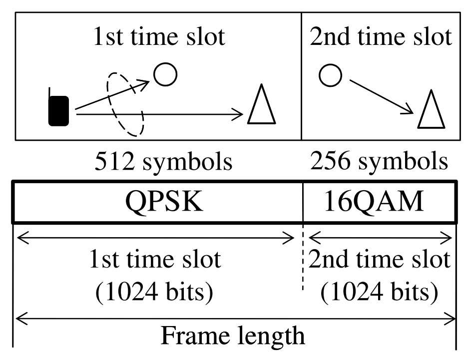

Fig. 3 A typical example of modulation combination for $K = 768$ symbols/frame.

In this paper, the best modulation combination to be stored in the look-up-table at BS will be found by the preliminary computer simulation (see Sect. 4.1).

Figure 2 shows the 2-time slot cooperative DF relay protocol. The first and second time slots constitute a frame of constant number of symbols. The frame length in symbols is denoted by K. The modulation levels may not necessarily be the same for the first and second time slots. Denoting the modulation level and number of symbols in the first (second) time slot by m_1 (m_2) and K_1 (K_2), respectively, we have

$$\begin{cases} m_1 K_1 = m_2 K_2 \\ K_1 + K_2 = K \end{cases} . \quad (2)$$

An example of modulation combination for the case of $K = 768$ symbols/frame is shown in Fig. 3.

The amount of data bits per frame which can be transferred from MT to BS is given by $Km_1m_2/(m_1+m_2)$ from Eq. (2). Assuming the selective repeat automatic repeat request (SR-ARQ), the throughput S is defined as

$$S = \frac{1}{1+N_g/N_c} \frac{m_1 m_2}{m_1+m_2} \{1 - PER(m_1, m_2)\} \text{(bps/Hz)}, \quad (3)$$

where $PER(m_1, m_2)$ denotes the packet error rate. N_c and N_g are the Fast Fourier transform (FFT) block size and the cyclic prefix (CP) length, respectively. The modulation combination is selected which maximizes S for the given MT-BS, MT-RS, and RS-BS links.

3. MMSE-FDE at RS and Signal Combining at BS

Since the modulation levels used in the first and second time slot may not be necessarily the same, an important issue is how to combine the signal received directly from MT (first time slot) and the one received via RS (second time slot). In this section, we present the signal combining method at BS.

Below, the symbol-spaced discrete-time signal representation is used.

3.1 Single-Carrier Transmission

During the first time slot, the data-modulated symbol sequence is divided into a sequence of N_c symbol blocks. The last N_g symbols of each N_c symbol block are inserted into the guard interval (GI) as CP. Then, MT broadcasts the sequence of CP-inserted symbol blocks to both RS and BS. RS applies MMSE-FDE to each CP-removed N_c symbol block and carries out the block data detection. During the second time slot, RS re-modulates the recovered data block and transmits it to BS after CP insertion. BS combines the signal blocks received from MT in the first time slot and RS in the second time slot.

The CP-removed received signal blocks at RS and BS in the first time slot are respectively denoted by $\{y_{M\to R}(t); t=0,\ldots,N_c-1\}$ and $\{y_{M\to B}(t); t=0,\ldots,N_c-1\}$. They can be expressed as

$$\begin{cases} y_{M\to R}(t) = \sqrt{2P_{M\to R}}\sum_{l=0}^{L-1} h_{M\to R}^{(l)} s_M\left(\left(t-\tau_{M\to R}^{(l)}\right) \bmod N_c\right) \\ \qquad + n_{M\to R}(t) \\ y_{M\to B}(t) = \sqrt{2P_{M\to B}}\sum_{l=0}^{L-1} h_{M\to B}^{(l)} s_M\left(\left(t-\tau_{M\to B}^{(l)}\right) \bmod N_c\right) \\ \qquad + n_{M\to B}(t) \end{cases}, \tag{4}$$

where $\{s_M(t); t=0,\ldots,N_c-1\}$ is the transmitted symbol block from MT. $h_{M\to B}^{(l)}$ is the complex-valued path gain of MT-BS link with $E\left[\sum_{l=0}^{L-1}\left|h_{M\to B}^{(l)}\right|^2\right]=1$. $\tau_{M\to R}^{(l)}$ and $\tau_{M\to B}^{(l)}$ are the time delays of the l-th path of the links between MT and RS and between MT and BS, respectively. $n_{M\to R}(t)$ and $n_{M\to B}(t)$ are the zero-mean complex-valued noise samples with variance $2\sigma_n^2 = 2N_0/T_s$, where T_s is the symbol duration and N_0 is the single-sided power spectrum density of the additive white Gaussian noise (AWGN). $P_{M\to B}$ and $P_{M\to R}$ are the local average received signal powers for the MT-BS and MT-RS links, respectively. They are given as

$$\begin{cases} P_{M\to B} = \bar{P}_M \cdot \bar{r}_{M\to B}^{-\alpha} \cdot 10^{-\eta_{M\to B}/10} \\ P_{M\to R} = \bar{P}_M \cdot \bar{r}_{M\to R}^{-\alpha} \cdot 10^{-\eta_{M\to R}/10} \end{cases}. \tag{5}$$

where $\bar{P}_M = P_M \cdot D^{-\alpha}$ is the normalized transmit power at MT with $\bar{r}_{M\to R} = r_{M\to R}/D$ and $\bar{r}_{M\to B} = r_{M\to B}/D$ being the normalized distances between MT and RS and between MT and BS, respectively. $\eta_{M\to B}$ is the independent log-normally distributed shadowing loss with standard deviation σ in dB for the MT-BS.

The CP-removed received signal blocks at BS in the second time slot is denoted by $\{y_{R\to B}(t); t=0,\ldots,N_c-1\}$. $y_{R\to B}(t)$ can be expressed as

$$y_{R\to B}(t) = \sqrt{2P_{R\to B}}\sum_{l=0}^{L-1} h_{R\to B}^{(l)} s_R\left(\left(t-\tau_{R\to B}^{(l)}\right) \bmod N_c\right) + n_{R\to B}(t), \tag{6}$$

where $\{s_R(t); t=0,\ldots,N_c-1\}$ is the transmitted symbol block from RS. $\tau_{R\to B}^{(l)}$ is the time delay of the RS-BS link. $n_{R\to B}(t)$ is the Gaussian noise with zero mean and variance $2N_0/T_s$ at BS during the second time slot. $P_{R\to B}$ is the local average received signal power for the RS-BS link and is given as

$$P_{R\to B} = \bar{P}_R \cdot \bar{r}_{R\to B}^{-\alpha} \cdot 10^{-\eta_{R\to B}/10}, \tag{7}$$

where $\bar{P}_R = P_R \cdot D^{-\alpha}$ is the normalized transmit power at RS, $\bar{r}_{R\to B} = r_{R\to B}/D$ is the normalized distance between RS and BS.

3.2 FDE at RS

Figure 4 illustrates the RS transceiver structure. The CP-removed received signal block $\{y_{M\to R}(t); t=0,\ldots,N_c-1\}$ is transformed by N_c-point fast Fourier transform (FFT) to the frequency-domain received signal $\{Y_{M\to R}(k); k=0,\ldots,N_c-1\}$. $Y_{M\to R}(k)$ is given as

$$\begin{aligned} Y_{M\to R}(k) &= \frac{1}{\sqrt{N_c}}\sum_{t=0}^{N_c-1} y_{M\to R}(t)\exp\left(-j2\pi k\frac{t}{N_c}\right) \\ &= H_{M\to R}(k)S_M(k) + \Pi_{M\to R}(k) \end{aligned}, \tag{8}$$

where

$$\begin{cases} S_M(k) = \frac{1}{\sqrt{N_c}}\sum_{t=0}^{N_c-1} s_M(t)\exp\left(-j2\pi k\frac{t}{N_c}\right) \\ H_{M\to R}(k) = \sqrt{2P_{M\to R}}\sum_{l=0}^{L-1} h_{M\to R}^{(l)}\exp\left(-j2\pi k\frac{\tau_{M\to R}^{(l)}}{N_c}\right) \\ \Pi_{M\to R}(k) = \frac{1}{\sqrt{N_c}}\sum_{t=0}^{N_c-1} n_{M\to R}(t)\exp\left(-j2\pi k\frac{t}{N_c}\right) \end{cases}. \tag{9}$$

Then, one-tap MMSE-FDE is applied as

$$\hat{Y}_{M\to R}(k) = Y_{M\to R}(k)W_{M\to R}(k), \tag{10}$$

where $W_{M\to R}(k)$ is the MMSE-FDE weight (which minimizes the mean square error (MSE) between $\hat{Y}_{M\to R}(k)$ and

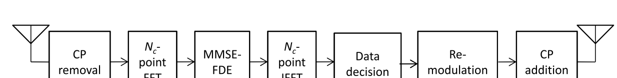

Fig. 4 RS structure.

$S_M(k)$) given as [5]

$$W_{M\to R}(k) = \frac{H^*_{M\to R}(k)}{|H_{M\to R}(k)|^2 + 2\sigma_n^2}, \tag{11}$$

where $(.)^*$ denotes the complex conjugate operation.

The frequency-domain signal $\left\{\hat{Y}_{M\to R}(k); k=0,\ldots,N_c-1\right\}$ after MMSE-FDE is transformed by N_c-point inverse FFT (IFFT) back to the time-domain signal block $\left\{\hat{d}_{M\to R}(t); t=0,\ldots,N_c-1\right\}$. $\hat{d}_{M\to R}(t)$ is given as

$$\begin{aligned}\hat{d}_{M\to R}(t) &= \frac{1}{\sqrt{N_c}}\sum_{k=0}^{N_c-1}\hat{Y}_{M\to R}(k)\exp\left(j2\pi t\frac{k}{N_c}\right)\\ &=\left(\frac{1}{N_c}\sum_{k=0}^{N_c-1}H_{M\to R}(k)W_{M\to R}(k)\right)s_M(t)\\ &\quad+\frac{1}{N_c}\sum_{k=0}^{N_c-1}H_{M\to R}(k)W_{M\to R}(k)\sum_{\tau=0\neq t}^{N_c-1}s_M(\tau)\exp\left(j2\pi k\frac{t-\tau}{N_c}\right)\\ &\quad+\frac{1}{N_c}\sum_{k=0}^{N_c-1}W_{M\to R}(k)\Pi_{M\to R}(k)\exp\left(j2\pi t\frac{k}{N_c}\right),\end{aligned} \tag{12}$$

where the first term is the desired signal and the second and third terms are respectively the residual inter-symbol interference (ISI) and the noise.

Finally, the data decision and data re-modulation is done to generate the symbol block $\{s_R(t); t=0,\ldots,N_c-1\}$, which is to be relayed to BS in the second time slot. In this paper, we consider the fixed DF relay protocol [3], in which RS transmits the re-modulated signal to BS in the second time slot even if data errors exist after decoding at RS.

3.3 Signal Combining at BS

Figure 5 illustrates the BS receiver structure. N_c-point FFT is applied to $\{y_{M\to B}(t); t=0,\ldots,N_c-1\}$ and $\{y_{R\to B}(t); t=0,\ldots,N_c-1\}$ to transform them into the frequency-domain received signals, $\{Y_{M\to B}(k); k=0,\ldots,N_c-1\}$ and $\{Y_{R\to B}(k); k=0,\ldots,N_c-1\}$, respectively. $Y_{M\to B}(k)$ and $Y_{R\to B}(k)$ are given as

$$\begin{cases} Y_{M\to B}(k) = \dfrac{1}{\sqrt{N_c}}\displaystyle\sum_{t=0}^{N_c-1}y_{M\to B}(t)\exp\left(-j2\pi k\frac{t}{N_c}\right)\\ \qquad\quad\;\; = H_{M\to B}(k)S_M(k) + \Pi_{M\to B}(k)\\ Y_{R\to B}(k) = \dfrac{1}{\sqrt{N_c}}\displaystyle\sum_{t=0}^{N_c-1}y_{R\to B}(t)\exp\left(-j2\pi k\frac{t}{N_c}\right)\\ \qquad\quad\;\; = H_{R\to B}(k)S_R(k) + \Pi_{R\to B}(k)\end{cases}, \tag{13}$$

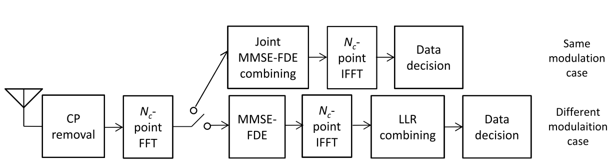

Fig. 5 BS receiver structure.

where

$$\begin{cases} S_R(k) = \dfrac{1}{\sqrt{N_c}}\displaystyle\sum_{t=0}^{N_c-1}s_R(t)\exp\left(-j2\pi k\frac{t}{N_c}\right)\\ H_{M\to B}(k) = \sqrt{2P_{M\to B}}\displaystyle\sum_{l=0}^{L-1}h^{(l)}_{M\to B}\exp\left(-j2\pi k\frac{\tau^{(l)}_{M\to B}}{N_c}\right)\\ H_{R\to B}(k) = \sqrt{2P_{R\to B}}\displaystyle\sum_{l=0}^{L-1}h^{(l)}_{R\to B}\exp\left(-j2\pi k\frac{\tau^{(l)}_{R\to B}}{N_c}\right)\\ \Pi_{M\to B}(k) = \dfrac{1}{\sqrt{N_c}}\displaystyle\sum_{t=0}^{N_c-1}n_{M\to B}(t)\exp\left(-j2\pi k\frac{t}{N_c}\right)\\ \Pi_{R\to B}(k) = \dfrac{1}{\sqrt{N_c}}\displaystyle\sum_{t=0}^{N_c-1}n_{R\to B}(t)\exp\left(-j2\pi k\frac{t}{N_c}\right)\end{cases}, \tag{14}$$

(a) In case of same modulation level

If the same data modulation level is used for both the first and second time slots, joint MMSE-FDE combining [5] is applied. The frequency-domain signal $\left\{\hat{Y}(k); k=0,\ldots,N_c-1\right\}$ after joint MMSE-FDE combining is given as

$$\hat{Y}(k) = Y_{M\to B}(k)W_{M\to B}(k) + Y_{R\to B}(k)W_{R\to B}(k), \tag{15}$$

where $W_{M\to B}(k)$ and $W_{R\to B}(k)$ are the MMSE weights which jointly minimizes the MSE between $\hat{Y}(k)$ and $S_M(k)$ and can be derived from [5] as

$$\begin{cases} W_{M\to B}(k) = \dfrac{H^*_{M\to B}(k)}{|H_{M\to B}(k)|^2 + |H_{R\to B}(k)|^2 + 2\sigma_n^2}\\ W_{R\to B}(k) = \dfrac{H^*_{R\to B}(k)}{|H_{M\to B}(k)|^2 + |H_{R\to B}(k)|^2 + 2\sigma_n^2}\end{cases}. \tag{16}$$

The frequency-domain signal $\left\{\hat{Y}(k); k=0,\ldots,N_c-1\right\}$ is transformed by N_c-point IFFT back to the time-domain signal $\left\{\hat{d}(t); t=0,\ldots,N_c-1\right\}$ as

$$\hat{d}(t) = \frac{1}{\sqrt{N_c}}\sum_{k=0}^{N_c-1}\hat{Y}(k)\exp\left(j2\pi t\frac{k}{N_c}\right). \tag{17}$$

(b) In case of different modulation levels

If the data-modulation level is different in the first and second time slots, the received signals from MT and RS are combined using log-likelihood ratio (LLR) combining [11] after MMSE-FDE. One-tap MMSE-FDE for $\{Y_{M\to B}(k); k=0,\ldots,N_c-1\}$ and $\{Y_{R\to B}(k); k=0,\ldots,N_c-1\}$ are given as

$$\begin{cases} \hat{Y}_{M\to B}(k) = Y_{M\to B}(k)W_{M\to B}(k)\\ \hat{Y}_{R\to B}(k) = Y_{R\to B}(k)W_{R\to B}(k)\end{cases}, \tag{18}$$

where $W_{M\to B}(k)$ and $W_{R\to B}(k)$ are the MMSE weights derived from [5] as

$$\begin{cases} W_{M\to B}(k) = \dfrac{H^*_{M\to B}(k)}{|H_{M\to B}(k)|^2 + 2\sigma_n^2}\\ W_{R\to B}(k) = \dfrac{H^*_{R\to B}(k)}{|H_{R\to B}(k)|^2 + 2\sigma_n^2}\end{cases}. \tag{19}$$

The frequency-domain signals $\left\{\hat{Y}_{M\to B}(k); k=0,\ldots,N_c-1\right\}$ and $\left\{\hat{Y}_{R\to B}(k); k=0,\ldots,N_c-1\right\}$ after MMSE-FDE are transformed by N_c-point IFFT back to the time-domain signals $\left\{\hat{d}_{M\to B}(t); t=0,\ldots,N_c-1\right\}$ and $\left\{\hat{d}_{R\to B}(t); t=0,\ldots,N_c-1\right\}$ as

$$\begin{cases} \hat{d}_{M\to B}(t) = \dfrac{1}{\sqrt{N_c}} \displaystyle\sum_{k=0}^{N_c-1} \hat{Y}_{M\to B}(k) \exp\left(j2\pi t \dfrac{k}{N_c}\right) \\ \hat{d}_{R\to B}(t) = \dfrac{1}{\sqrt{N_c}} \displaystyle\sum_{k=0}^{N_c-1} \hat{Y}_{R\to B}(k) \exp\left(j2\pi t \dfrac{k}{N_c}\right) \end{cases}, \tag{20}$$

from which the bit-LLRs, $\lambda_{M\to B,x}(t)$ and $\lambda_{R\to B,x}(t)$ of x-th bit within t-th symbol, are computed using [11]

$$\begin{cases} \lambda_{M\to B,x}(t) = \left(\begin{array}{l} \left| \hat{d}_{M\to B}(t) - \dfrac{1}{N_c}\displaystyle\sum_{k=0}^{N_c-1} \hat{H}_{M\to B}(k) d^{\min}_{M\to B,b(x)=0} \right|^2 \\ - \left| \hat{d}_{M\to B}(t) - \dfrac{1}{N_c}\displaystyle\sum_{k=0}^{N_c-1} \hat{H}_{M\to B}(k) d^{\min}_{M\to B,b(x)=1} \right|^2 \end{array} \right) \\ \lambda_{R\to B,x}(t) = \left(\begin{array}{l} \left| \hat{d}_{R\to B}(t) - \dfrac{1}{N_c}\displaystyle\sum_{k=0}^{N_c-1} \hat{H}_{R\to B}(k) d^{\min}_{R\to B,b(x)=0} \right|^2 \\ - \left| \hat{d}_{R\to B}(t) - \dfrac{1}{N_c}\displaystyle\sum_{k=0}^{N_c-1} \hat{H}_{R\to B}(k) d^{\min}_{R\to B,b(x)=1} \right|^2 \end{array} \right) \end{cases}, \tag{21}$$

where

$$\begin{cases} \hat{H}_{M\to B}(k) = H_{M\to B}(k) W_{M\to B}(k) \\ \hat{H}_{R\to B}(k) = H_{R\to B}(k) W_{R\to B}(k) \end{cases}. \tag{22}$$

In Eq. (21), $d^{\min}_{M\to B,b(x)=0(1)}$ and $d^{\min}_{R\to B,b(x)=0(1)}$ are the symbol candidates which have the maximum LLR within the set of the data symbols. $2\sigma^2_{M\to B}$ and $2\sigma^2_{R\to B}$ are the sum variances of the residual ISI and the noise given as

$$\begin{cases} 2\sigma^2_{M\to B} = \dfrac{1}{N_c}\displaystyle\sum_{k=0}^{N_c-1} \left|\hat{H}_{M\to B}(k)\right|^2 - \left|\dfrac{1}{N_c}\displaystyle\sum_{k=0}^{N_c-1} \hat{H}_{M\to B}(k)\right|^2 \\ \qquad + \dfrac{2\sigma_n^2}{N_c}\displaystyle\sum_{k=0}^{N_c-1} |W_{M\to B}(k)|^2 \\ 2\sigma^2_{R\to B} = \dfrac{1}{N_c}\displaystyle\sum_{k=0}^{N_c-1} \left|\hat{H}_{R\to B}(k)\right|^2 - \left|\dfrac{1}{N_c}\displaystyle\sum_{k=0}^{N_c-1} \hat{H}_{R\to B}(k)\right|^2 \\ \qquad + \dfrac{2\sigma_n^2}{N_c}\displaystyle\sum_{k=0}^{N_c-1} |W_{R\to B}(k)|^2 \end{cases}. \tag{23}$$

The LLR combining to obtain the LLR λ_x for x-th bit is given as

$$\lambda_x = \lambda_{M\to B,x_1}(t_1) + \lambda_{R\to B,x_2}(t_2), \tag{24}$$

where $\lambda_{M\to B,x_1}(t_1)$ is the LLR of the x_1-th bit of the t_1-th symbol in the time-domain signal received from MT and $\lambda_{R\to B,x_2}(t_2)$ is the LLR of the x_2-th bit of the t_2-th symbol in the time-domain signal received from RS. Note that the following relationship between λ_x, $\lambda_{M\to B,x_1}(t_1)$ and $\lambda_{R\to B,x_2}(t_2)$ holds:

$$x = x_1 + m_1 t_1 = x_2 + m_2 t_2. \tag{25}$$

In Eq. (24), if λ_x is positive (negative), the x-th transmit bit is determined as 1 (0).

4. Computer Simulation

The simulation condition is shown in Table 1. We want to discuss the behavior of the adaptive modulation. In the computer simulation, we consider 3 modulation modes, BPSK, QPSK and 16QAM only and the uncoded transmission. Therefore, there exist nine possible modulation combinations shown in Table 2. A frequency-selective block Rayleigh fading channel having a symbol-spaced L=16-path uniform power delay profile is assumed. In this paper, we assume that the frame length is kept constant, but the ratio of first and second time slot lengths is changed according to the modulation levels used in the first and second time slots. The frame length is kept constant irrespective of the modulation combination. Therefore, the frame length should be a common multiple of block size N_c and the first time slot-to-frame length ratio $m_1/(m_1+m_2)$. In the computer simulation, we assume N_c=256 and consider BPSK, QPSK, and 16QAM data modulation (i.e., $m_1/(m_1+m_2)$=2, 3, 4, and 5). Therefore, the frame length is set to 30720 symbols, which is the least common multiple of N_c=256 and $m_1/(m_1+m_2)$=2, 3, 4, and 5. Figure 6 illustrates the single-cell/single-user relay network model assumed for computer simulation. It is assumed that 6 RSs are located equal-distantly to each other at the normalized distance $r_{R\to B}/D$ = 0.5 from BS. MT location is randomly selected within the cell. The normalized total transmit power $\bar{P}=P\cdot D^{-\alpha}$ is assumed to be equally allocated to MT and RS as $\bar{P}_M=\bar{P}_R=\bar{P}/2$.

Table 1 Simulation condition.

Transmission data	Block size	N_c = 256
	CP length	N_g = 16
	Frame size	K = 30720(symbols)
Channel	Fading type	Block Rayleigh fading
	Power delay profile	Uniform
	No. of paths	L = 16
	Path loss exponent	α = 3.5
	Shadowing loss standard deviation of MT-RS link	σ = 7.0(dB)
RS Receiver	Equalization	MMSE-FDE
	Channel estimation	Ideal
BS Receiver	Equalization	MMSE-FDE
	Combining scheme	MMSE-FDE combining, LLR combining
	Channel estimation	Ideal

Table 2 Possible modulation combinations. (Modulation1-Modulation2)

BPSK-BPSK	BPSK-QPSK	BPSK-16QAM
QPSK-BPSK	QPSK-QPSK	QPSK-16QAM
16QAM-BPSK	16QAM-QPSK	16QAM-16QAM

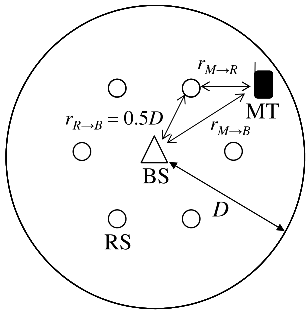

Fig. 6 Network model for computer simulation.

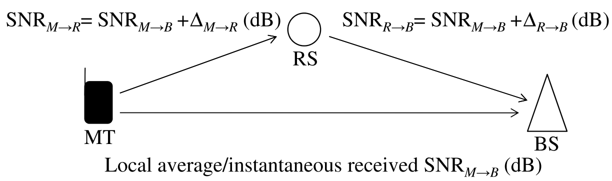

Fig. 7 Simulation model.

4.1 Fiding the Best Modulation Combination

The best modulation combination was found by preliminary computer simulation. Figure 7 illustrates the simulation model. It is assumed that the local average/instantaneous received SNRs of MT-RS and RS-BS links are different by $\Delta_{M\to R}$ and $\Delta_{R\to B}$ dB, respectively, from the local average/instantaneous received SNR ($SNR_{M\to B}$) of MT-BS link.

Figures 8(a) and (b) show the best modulation combination when the local average received $SNR_{M\to B}$=5 dB and 10 dB, respectively. It should be noted that the same amount of data bits must be transmitted in the first and second time slots. It can be seen from Figs. 8(a)(b) that, when the MT-RS link has better channel quality than the RS-BS link, more transmission time is given to the second time slot by using higher modulation level in the first time slot (MT-RS transmission). It can be seen from Fig. 8(a) that when $\Delta_{M\to R}$ ($\Delta_{R\to B}$) is high, higher level modulation is used in the first (second) time slot.

For comparison, the best modulation combination found when the instantaneous received $SNR_{M\to B}$=5 and 10 dB is shown in Figs. 8(c) and (d), respectively. Comparison between Figs. 8(a)(b) and Figs. 8(c)(d) shows that the best modulation combination based on the instantaneous received SNRs differs only slightly from that based on the local average received SNRs. This is because, in a strong frequency-selective fading channel, the instantaneous received SNR varies only slightly and approaches the local average received SNR (see Appendix). Therefore, in the following simulation, the modulation combination found based on the local average received SNR is used.

4.2 Throughput Performance

The average throughput S is computed as

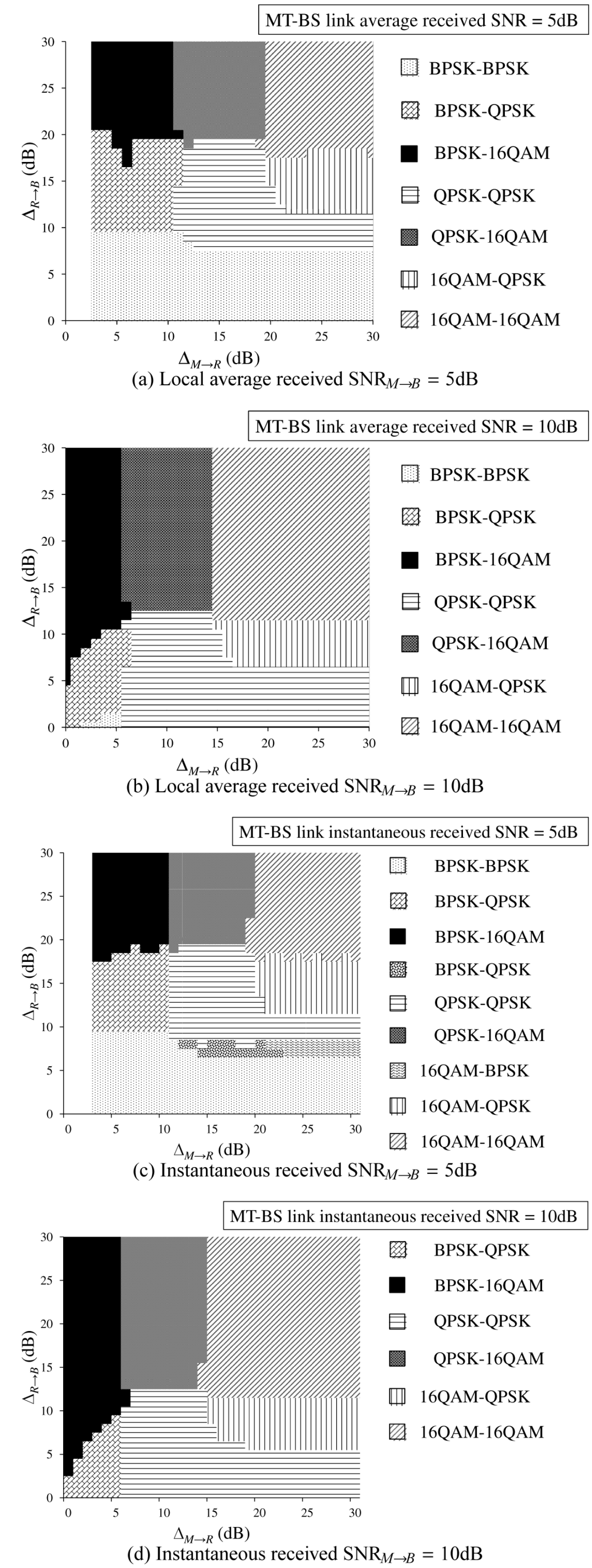

Fig. 8 Best modulation combination.

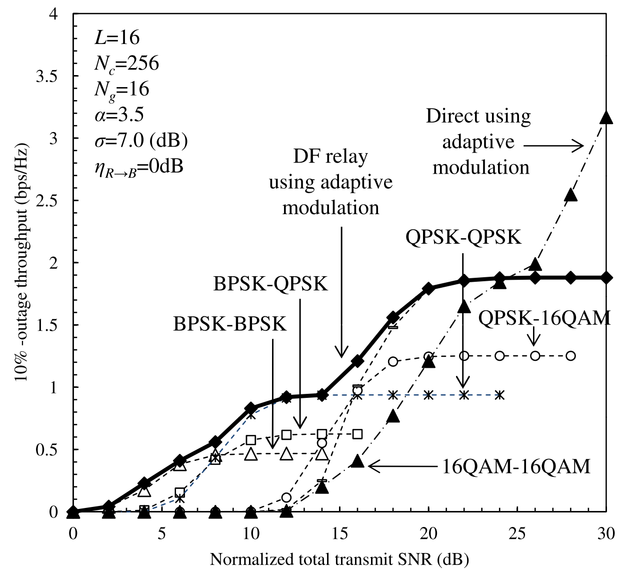

Fig. 9 10%-outage throughput performance.

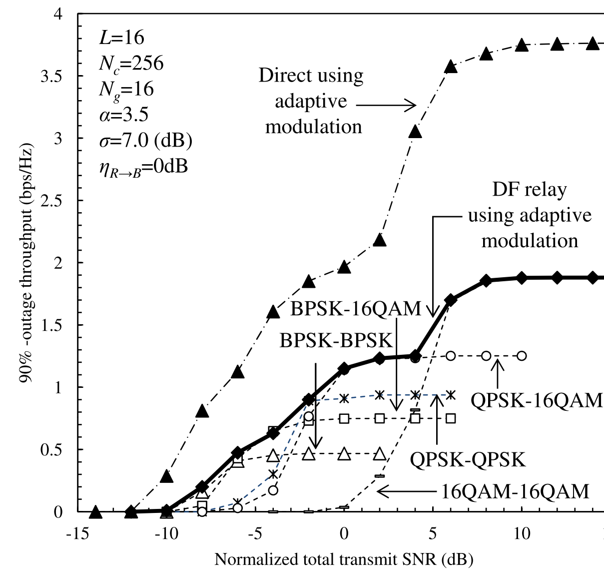

Fig. 10 90%-outage throughput performance.

$$S = \frac{1}{1+N_g/N_c}\sum_{a=0}^{A-1} p_a \left\{\frac{m_{a,1}m_{a,2}}{m_{a,1}+m_{a,2}}(1-PER_a)\right\} (\text{bps/Hz}), \quad (26)$$

where p_a is the probability that the a-th($a=0,\ldots,A$–1) modulation combination is selected, A is the number of possible modulation combinations, and PER_a, $m_{a,1}$ and $m_{a,2}$ are respectively the PER and the number of bits per symbol in the first and second time slots when the a-th modulation combination is used.

Figure 9 plots the 10%-outage throughput (below which the measured throughput falls with the probability of 10%) as a function of the normalized total transmit SNR ($\bar{P}/\sigma_n$) when the shadowing loss of RS-BS link $\eta_{R\to B}=0$ dB. For comparison, the 10%-outage throughput of 2-time slot cooperative DF relay using fixed modulation combination is also plotted as the dashed line and that of direct communication using adaptive modulation as the dashed-dotted line. The use of adaptive modulation can achieve higher throughput than fixed modulation. The throughput of direct communication using adaptive modulation is lower than cooperative DF relay using adaptive modulation when the transmit SNR<24 dB. The cooperative DF relay using adaptive modulation reduces by about 9 dB the required SNR for a throughput of 0.8 bps/Hz compared to direct transmission. This is because 10%-outage throughput represents the throughput of a user close to the cell-edge (i.e., the MT-BS link is in a poor condition).

Figure 10 plots the 90%-outage throughput (below which the throughput falls with the probability of 90%) using adaptive modulation when the shadowing loss of RS-BS link $\eta_{R\to B}$=0 dB. For comparison, the 90%-outage throughput of cooperative DF relay using fixed modulation combination is also plotted as the dashed lines and that of direct communication using adaptive modulation as the dashed-dotted line. The 90%-outage throughput of direct communication always achieves higher throughput than that of cooperative DF relay using adaptive modulation. This is because 90%-outage throughput represents the throughput of a user close to the center of the cell (i.e., the MT-BS link is in a good condition) and thus, the loss of using 2-time slot relay offsets the spatial diversity gain.

5. Conclusion

In this paper, we introduced the adaptive modulation to 2-time slot uplink SC cooperative DF relay. It was confirmed by computer simulation that cooperative DF relay with adaptive modulation can achieve higher throughput than cooperative DF relay with fixed modulation. However, even if adaptive modulation is used, the throughput of 2-time slot cooperative DF relay degrades compared to direct communication when the MT-BS link is in a good condition (e.g., when MT is close to the center of the cell). Switching between cooperative DF relay and direct communication may always achieve better throughput. This is left as our future work.

Adaptive modulation requires that BS knows the CSIs of MT-BS, MT-RS, and RS-BS links, selects the best modulation combination from the look-up table, and informs the best modulation combination to both MT and RS. How to implement this is an important practical issue and is left as our future study. In the computer simulation, we considered only 3 modulation modes, the uncoded transmission, and equal power allocation. More general adaptive modulation and coding and adaptive power allocation for SC cooperative DF relay are left as our future work.

References

[1] W.C. Jakes, Jr., Ed., Microwave Mobile Communications, Wiley, New York, 1974.
[2] R. Pabst, B.H. Walke, D.C. Schultz, P. Herhold, H. Yanikomeroglu, S. Mukherjee, H. Viswanathan, M. Lott, W. Zirwas, M. Dohler,

H. Aghvami, D.D. Falconer, and G.P. Fettweis, "Relay-based deployment concepts for wireless and mobile broadband radio," IEEE Commun. Mag., vol.42, no.9, pp.80–89, Sept. 2004.

[3] J.N. Laneman, D.N.C. Tse, and G.W. Wornell, "Cooperative diversity in wireless networks: Efficient protocols and outage behavior," IEEE Trans. Inf. Theory, vol.50, no.12, pp.3062–3080, Dec. 2004.

[4] D. Falconer, S.L. Ariyavisitakul, A. Benyamin-Seeyar, and B. Eidson, "Frequency domain equalization for single-carrier broadband wireless systems," IEEE Commun., vol.40, no.4, pp.58–66, April 2002.

[5] F. Adachi and T. Sao,"Joint antenna diversity and frequency-domain equalization for multi-rate MC-CDMA," IEICE Trans. Commun., vol.E86-B, no.11, pp.3217–3224, Nov. 2003.

[6] Z. Lin and E. Erkip, "Adaptive modulation for coded cooperative systems," Proc. IEEE SPAWC, pp.615–619, June 2005.

[7] A.B. Sediq and H. Yanikomeroglu, "Performance analysis of SNR-based selection combining and BER-based selection combining of signals with different modulation levels in cooperative communications," Proc. IEEE VTC09-Fall, pp.1–5, Anchorage, Sept. 2009.

[8] Y. Luo and L. Cai, "Throughout maximization for user cooperative wireless systems with adaptive modulation," Commun. (ICC), 2010 IEEE International Conference, pp.1–5, Canada, May 2010.

[9] Y. Ma, R. Tafazolli, Y. Zhang, and C. Qian, "Adaptive modulation for opportunistic decode-and-forward relaying," IEEE Trans. Wireless Commun., vol.10, no.7, pp.2017–2022, July 2011.

[10] S.S. Ikki, O. Amin, and M. Uysal, "Performance analysis of adaptive L-QAM for oppotunistic decode-and-forward relaying," Proc. IEEE VTC10-Spring, pp.1–5, May 2010.

[11] A. Stefanov and T. Duman, "Turbo coded modulation for wireless communications with antenna diversity," Proc. IEEE VTC99-Fall, pp.1565–1569, Netherland, Sept. 1999.

[12] J.G. Proakis, Digital Communications, 2nd ed., McGraw-Hill, 1995.

[13] K. Kimura, M. Nakada, T. Obara, and F. Adachi, "Single-carrier cooperative DF relay using adaptive modulation," Proc. 8th Asia Pacific Wireless Communication Symposium (APWCS2011), Singapore, Aug. 2011.

Appendix: Variation of Instantaneous SNR

Assuming a frequency-selective Rayleigh channel and uniform power delay profile, the instantaneous SNR γ_{inst} is given as

$$\gamma_{inst} = \frac{P_{ave}}{\sigma_n^2} \sum_{l=0}^{L-1} |h_l|^2 = \gamma_{ave} \cdot Z, \tag{A$\cdot$1}$$

where $\gamma_{ave} = P_{ave}/\sigma_n^2$ is the local average received SNR with denoting P_{ave} and σ_n^2 as the local average received power and the noise power, respectively. h_l denotes the zero-mean complex valued l-th path gain with $E\left[\sum_{l=0}^{L-1} |h_l|^2\right] = 1$, where $E[.]$ denotes the ensemble average operator. In this paper, the uniform power delay profile (i.e., $E\left[|h_l|^2\right] = 1/L$) is assumed and hence, the sum of squared path gains, $Z = \sum_{l=0}^{L-1} |h_l|^2$, follows a χ^2-distribution with $2L$ degree-of-freedom. The probability density function (PDF) of Z is given as [12]

$$p(Z) = \frac{L^L}{\Gamma(L)} Z^{L-1} e^{-ZL}, \tag{A$\cdot$2}$$

where $\Gamma(.)$ denotes the gamma function. The mean $E(Z) = 1$ and the variance $V(Z) = 1/L$. As L increases, $V(Z)$ gets smaller and as a consequence, the instantaneous received SNR approaches the local average received SNR.

Kazuhiro Kimura received his B.S. degree in Information and Intelligent Systems from Tohoku University, Sendai Japan, in 2011. Currently he is a graduate student at the Department of Communications Engineering, Graduate School of Engineering, Tohoku University. His research interests include cooperative decode-and-forward relay and adaptive modulation.

Hiroyuki Miyazaki received his B.S. degree in Information and Intelligent Systems from Tohoku University, Sendai Japan, in 2011. Currently he is a graduate student at the Department of Communications Engineering, Graduate School of Engineering, Tohoku University. His research interests include cooperative amplify-and-forward relay and network coding systems.

Tatsunori Obara received his B.S. degree in Electrical, Information and Physics Engineering in 2008 and M.S. degree in communications engineering, in 2010, respectively, from Tohoku University, Sendai Japan. Currently he is a Japan Society for the Promotion of Science (JSPS) research fellow, studying toward his PhD degree at the Department of Electrical and Communications Engineering, Graduate School of Engineering, Tohoku University. His research interests include channel equalization techniques for mobile communication systems.

Fumiyuki Adachi received the B.S. and Dr. Eng. degrees in electrical engineering from Tohoku University, Sendai, Japan, in 1973 and 1984, respectively. In April 1973, he joined the Electrical Communications Laboratories of Nippon Telegraph & Telephone Corporation (now NTT) and conducted various types of research related to digital cellular mobile communications. From July 1992 to December 1999, he was with NTT Mobile Communications Network, Inc. (now NTT DoCoMo, Inc.), where he led a research group on wideband/broadband CDMA wireless access for IMT-2000 and beyond. Since January 2000, he has been with Tohoku University, Sendai, Japan, where he is a distinguished Professor of Communications Engineering at the Graduate School of Engineering. His research interest is in the areas of wireless signal processing and networking including broadband wireless access, equalization, transmit/receive antenna diversity, MIMO, adaptive transmission, channel coding, etc. He was a program leader of the 5-year Global COE Program "Center of Education and Research for Information Electronics Systems" (2007–2011), awarded by the Ministry of Education, Culture, Sports, Science and Technology of Japan. From October 1984 to September 1985, he was a United Kingdom SERC Visiting Research Fellow in the Department of Electrical Engineering and Electronics at Liverpool University. He is an IEICE Fellow and was a co-recipient of the IEICE Transactions best paper of the year award 1996, 1998, and 2009 and also a recipient of Achievement award 2003. He is an IEEE Fellow and a VTS Distinguished Lecturer for 2011 to 2013. He was a co-recipient of the IEEE Vehicular Technology Transactions best paper of the year award 1980 and again 1990 and also a recipient of Avant Garde award 2000. He was a recipient of Thomson Scientific Research Front Award 2004, Ericsson Telecommunications Award 2008, Telecom System Technology Award 2009, and Prime Minister Invention Prize 2010.